

A review of synergy concepts of nonlinear blending and dose-reduction profiles

John J. Peterson

Drug Development Sciences Department, Research Statistics Unit (UP-4315), GlaxoSmithKline Pharmaceuticals, R&D, 1250 So. Collegeville Road, Collegeville, Pennsylvania 19426, USA

TABLE OF CONTENTS

1. Abstract
2. Introduction
 - 2.1. Two classical approaches to synergy
 - 2.2. A nonlinear blending approach to drug synergy
 - 2.3. A dose reduction profile approach to compound blending
3. Response surface modeling
 - 3.1. The molar-unit Minto-White model
 - 3.2. Low folic acid experiment
 - 3.3. High folic acid experiment
4. Nonlinear blending analysis
 - 4.1. Strong nonlinear blending
 - 4.2. Low folic acid experiment
 - 4.3. High folic acid experiment
5. Analysis of dose reduction profiles
 - 5.1. Dose reduction profile curves
 - 5.2. Low folic acid experiment
 - 5.3. High folic acid experiment
6. Summary and perspective
7. Acknowledgements
8. References

1. ABSTRACT

This article presents a case-study review of synergy concepts of nonlinear blending and dose-reduction profiles. “Strong nonlinear blending” is a novel concept that provides a flexible paradigm for the assessment of combination drug synergy that is applicable to any shaped combination-drug dose-response surface; issues of varying relative potency, partial inhibitors, potentiation, or coalism pose no problems at all. Dose-reduction profiles are overlay plots created to show how much each drug can be reduced in amount and yet achieve the same efficacy as larger amounts of each drug used individually. This review applies these synergy concepts to two data sets from a previously published experiment. The previous publication had claimed a high degree of Loewe synergy for one of the data sets. However, a more penetrating analysis shows that with regard to strong nonlinear blending there is no reason to blend (for purposes of response enhancement) the two compounds studied. However, the dose-reduction profile plots show how Loewe synergy is present and provide further insight to the interaction of the two compounds (on the dose-concentration scale).

2. INTRODUCTION

This article presents two dose-response surface analyses of combinations of trimetrexate (TMQ) and a compound known as AG2034 in the presence of low and high levels of folic acid, respectively. The data come from an experiment published by Faessel *et al.* (1). The dose-response surface models are obtained using a modified version of the hierarchical logistic modeling approaches appearing in Minto *et al.* (2) and White *et al.* (3). Using these dose-response models, an investigation of possible drug synergy is performed using a methodology based upon mixture-amount experiments. Within the framework of mixture-amount experiments, the concept of “strong nonlinear blending” is applied to these hierarchical models to assess these experiments for the presence of combination drug synergy. Strong nonlinear blending is a novel synergy concept first appearing in Peterson and Novick (4). It provides a very flexible paradigm for the assessment of combination drug synergy that is applicable to any shaped combination-drug dose-response surface; issues of varying relative potency, partial inhibitors, potentiation, or coalism pose no problems at all.

The nonlinear blending analysis shows that there is little or nothing to be gained in response improvement by blending AG2034 with TMQ. In most cases, replacing TMQ molecules with AG2034 molecules simply dilutes the combination drug effect in the sense that there is insufficient Loewe synergy to overcome the loss of efficacy obtained by adding the less potent AG2034.

As a secondary analysis, a series of "dose reduction profile" plots are created. These plots are created to show how much each drug can be reduced in amount and yet achieve the same efficacy as larger amounts of each drug used individually. While this is not a synergy analysis on the response scale, such an analysis may nonetheless have utility in situations where smaller amounts of two drugs used together produce less frequent or less serious adverse reactions than larger amounts of either drug used one alone. For the combination drug experiment in the presence of high folic acid, it does appear that the blending of AG2034 and TMQ offers excellent dose reduction potential.

The dose-response modeling for the two TMQ-AG2034 data sets is described in section 3. The nonlinear blending analyses are provided in section 4, while section 5 describes the dose reduction profile analyses. A summary is given in section 6. Subsection 2.1 below describes two classical approaches to quantifying combination drug synergy, while subsection 2.2 introduces the approach of nonlinear blending found in the area of mixture amount experiments. Section 2.3 discusses the graphical concept of "dose reduction profile" plots.

2.1. Two classical approaches to synergy

As a precursor to the synergy analyses in section 4, it may be helpful to the reader, particularly one who is more familiar with the classical approaches to synergy quantification, to understand why the approach of nonlinear blending (more widely known in agriculture and industrial settings) is favored by this author as a general approach to drug synergy quantification on the response scale. The reader may better understand the rationale for the nonlinear blending approach by taking notice of the weaknesses inherent in the classical approaches to drug synergy quantification and then make comparisons with the more widely applicable approach of strong nonlinear blending.

In this introduction, I will briefly review the two most widely used classical approaches to quantifying combination drug synergy, Bliss independence (5) and Loewe synergy (6). The Bliss independence model assumes that both drugs act independently on different targets. The Bliss independence model can be described as follows. Suppose that drug 1 produces a "fraction of possible response", f_1 at amount A_1 , drug 2 produces a fraction of possible response, f_2 at A_2 , and a combination of drugs 1 and 2 produces a "fraction of possible response", f_{12} , at amount $(A_1 + A_2)$. The Bliss independence model states that then the fraction of possible response produced by drugs 1 and 2 combined is $f_{12} = f_1 + f_2 - f_1 f_2$ (Suppose that it is assumed that a larger response is better.)

If instead $f_{12} > f_1 + f_2 - f_1 f_2$, then we have Bliss synergy; likewise if $f_{12} < f_1 + f_2 - f_1 f_2$, then we have Bliss antagonism.

As shown by Greco *et al.* (7), the Bliss independence concept exhibits a troubling aspect of quantification when viewed along a dose-response continuum. For example, assume that $f_1(\frac{1}{2}A) = 0.1$, $f_2(\frac{1}{2}A) = 0.1$ and $f_{12}(\frac{1}{2}A, \frac{1}{2}A) = 0.4$. One would then conclude Bliss synergy at $(\frac{1}{2}A, \frac{1}{2}A)$ since $0.4 > 0.19$. However, suppose $f_1(A) = 0.6$ and $f_2(A) = 0.6$. In this case one has to admit that a total amount, A , of either drug 1 or drug 2 *alone* produces a better response than the combination total amount, A , of drugs 1 and 2 together, despite Bliss synergy.

Loewe synergy (6) is based upon the "sham experiment" concept. This concept says that a drug combined with itself must be additive. This idea can be extended to two different compounds with the same relative potency, i.e. the same shape on the log-dose scale. Suppose that drug 2 has the smaller IC_{50} . Dilute drug 2 until both dose response curves completely overlap. Call the diluted form of drug 2, drug 2'. If the response surface for the combinations of drug 1 and drug 2' is the same as that for the combinations of drug 1 and drug 1 (or equivalently for drug 2' and drug 2') then we have Loewe additivity (also called dosewise additivity). Under these assumptions, one can derive the familiar equation for dosewise additivity,

$$\frac{d_1}{IC_{50}^{(1)}} + \frac{d_2}{IC_{50}^{(2)}} = 1,$$

where $IC_{50}^{(1)}$ and $IC_{50}^{(2)}$ are the IC_{50} 's for drugs 1 and 2 respectively. There are several derivations in the literature. See for example, Loewe (6), Greco *et al.* (7), Tallarida (8), or Peterson and Novick (4).

The sham experiment paradigm appears to be a solid one, but only for compounds with *constant* relative potency. If, however, two compounds have varying relative potencies, then one cannot dilute the more potent one to make both dose response curves completely overlap so as to allow a comparison with the sham experiment. In fact, some authors have tried to apply the dosewise additive argument to compounds with differing relative potencies and noted that such a derivation produces odd results, such as two different curvilinear isobolograms. Peterson and Novick (4) show that the sham experiment strategy can lead to paradoxical results, and simply does not make sense, whenever two drugs do not have the same relative potency, i.e. the exact same shape on the log-dose scale.

However, even if we restrict ourselves to dose response curves with the same shape on the log-dose scale, the Loewe synergy concept can be misleading when the two compounds have very different potencies. In fact, it is

possible for a 50-50 blend of two compounds to show Loewe synergy yet this blend has an IC_{50} much larger than the IC_{50} of the more potent compound. (Here, IC_{50} is defined as the concentration of a drug that produces a 50% mean inhibition or 50% reduction from mean baseline response.)

As an example, following Berenbaum (9), define the interaction index, I , as

$$I = \frac{d_1}{IC_{50}^{(1)}} + \frac{d_2}{IC_{50}^{(2)}}.$$

If $I < 1$ then drugs 1 and 2 are said to be Loewe synergistic. If $I = 1$, then drugs 1 and 2 are said to be Loewe additive. If $I > 1$, then drugs 1 and 2 are said to be Loewe antagonistic.

Suppose that $IC_{50}^{(1)} = 1$, $IC_{50}^{(2)} = 50$, and the combination, $d_1 = 0.1$, $d_2 = 9.9$, produces a 50% response. It follows then that the interaction index, I , is 0.298. Interaction indices having a value of 0.7 or less are generally considered to be substantially synergistic (10). So $I = 0.298$ states strong synergy for the dose combination, $(d_1, d_2) = (0.1, 9.9)$. However, the total dose for this combination is $d_1 + d_2 = 10$. But, this is a

10-fold increase over $IC_{50}^{(1)}$ which is equal to 1. So, the combination drug (along a fixed-dose-ratio ray of $100d_1 / (d_1 + d_2)\%$ of drug 1) has an IC_{50} (on that ray) much larger than the best single drug IC_{50} despite having a very synergistic interaction index value. A graphical description (not to scale) of this phenomenon for Loewe synergy can be found in Figure 5A.

Some researchers have also been known to modify the interaction index I above by defining the IC_{50} to instead be the inflection point on the (logistic model) Hill equation on the log-dose scale, i.e. the point associated with a mean response halfway between the upper and lower asymptotes of the log-dose curve. Unfortunately, this approach can also produce troubling results with regard to synergy quantification when applied to partial inhibitors or partial agonists. For example, suppose that compounds 1 and 2 have mean (inhibition) dose response curves given by

$$f_1(d_1) = 0.7 + 0.3 / (1 + 10^{\log_{10}(d_1)}) \quad \text{and} \quad f_2(d_1) = 0.7 + 0.3 / (1 + 10^{(\log_{10}(d_2)-1)}) , \quad \text{respectively.}$$

In this case, compound 1 has an (inflection point) IC_{50} of 1 and compound 2 has an (inflection point) IC_{50} of 10. Suppose further that along a fixed-dose-ratio ray of, say, a 50:50 combination of compounds 1 and 2, we have the dose response curve, $f_{12}(d_1, d_2) = 1 / (1 + 10^{[(\log_{10}(d_1+d_2)-1.5)/2]})$. As such, along this 50:50 dose-ratio-ray, the combination has an (inflection point) IC_{50} of $10^{1.5} = 31.6$. Suppose that this IC_{50} of 31.6 is achieved with individual doses of $d_1 = 15.8$ and $d_2 = 15.8$. This corresponds to an interaction index of $I =$

$(15.8/1) + (15.8/10) = 17.38$, which is a highly antagonistic index value. However, consider the overlay plot of all three of these curves vs. log-total-dose is given in Figure 1. Here, one can readily see that we have in fact a synergistic drug combination rather than a highly antagonistic one, as the interaction index would imply.

In a report of the International Union of Pure and Applied Chemistry, Lehár and Keith (11) stated that many observed combination drug effects defy description by either of the accepted standard models (Bliss or Loewe). They stated:

“Rather than simply exceeding or falling short of one of the standards, many observed effects alternate between synergy and antagonism depending on the relative concentrations of the compounds. The standard reference models also can't describe coalism effects, where two inactive agents give rise to a combined effect that could never be predicted from the single agent dose responses. Evidently, the standard combination references cannot account for the wide variety of empirical contexts.”

Hence, it is clear that a more widely applicable approach to quantifying combination drug synergy is needed. One such approach can be found in the subject of "mixture amount experiments".

2.2. A nonlinear blending approach to drug synergy

The subject of "mixture experiments" deals with modeling the responses obtained from the blending of various substances. Two books devoted to this area are by Cornell (12) and Smith (13). Most of the literature on mixture experiments assumes that the blending properties of the substances being combined are not affected by the total amount of substance used. This would be the case for mixture experiments involving blending of substances such as paint, gasoline, soft drinks, etc. However, experiments where the total amount of substance, as well as the mixing proportions, affect the response are called "mixture amount" experiments (14,15). While mixture amount experiments have been successfully used in both agricultural (e.g. fertilizer blending) and industrial settings (e.g. mineral processing) their first apparent use was in an assessment of drug synergy (16). In fact, mixture-amount experiments are a natural way to think about combination-drug dose-response experiments. Two recent papers on applications of mixture-amount experiments to cancer drug modeling are by Kitsos and Edler (17) and Chen *et al.* (18).

For a fixed total amount, A , of k blended substances, one can define a mixture-amount model as

$$y = m(\mathbf{x}, A; \boldsymbol{\beta}) + e ,$$

where y is the response and m is the mean response surface function of $\mathbf{x} = (x_1, \dots, x_k)$ and A , the k mixing proportions and the total amount of drug substance, respectively.

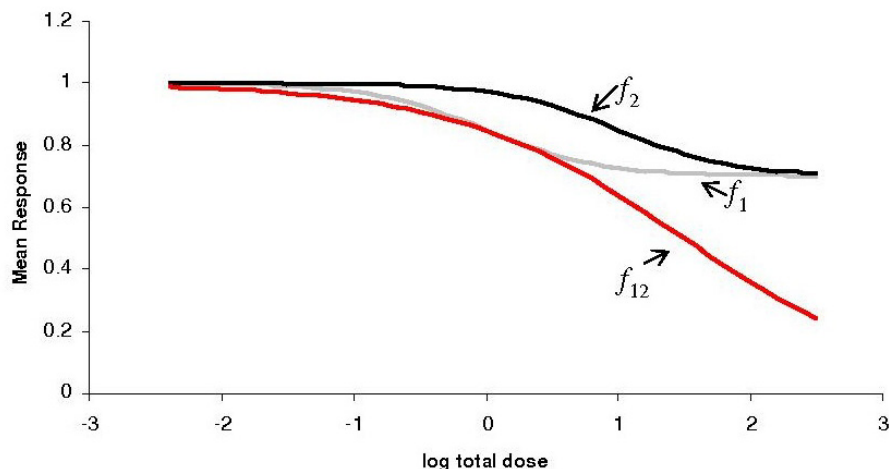


Figure 1. The curve traced out in red is the dose response curve corresponding to the 50:50 compound combination. The black and gray dose response curves correspond to the single drugs.

Here, $\beta = (\beta_1, \dots, \beta_t)$ is a vector of regression parameters and e denotes the random error deviation of the mean response surface function, m , from the measured response, y . A key assumption of a mixture or mixture-amount experiment is that all of the x -variables (proportions) sum to 1, i.e. $x_1 + \dots + x_k = 1$. The actual dose, d_i , of drug i in any combination is $d_i = x_i A$ ($i = 1, \dots, k$), which of course implies that $d_1 + \dots + d_k = A$. The response surface function, m , can be completely general, determined empirically or mechanistically.

For simplicity, consider only two drugs, 1 and 2. A simple quadratic-form mixture-amount model is:

$$m(x, A, \beta) = \beta_1(A)x_1 + \beta_2(A)x_2 + \beta_{12}(A)x_1x_2,$$

where each β -regression coefficient depends upon A , the total dose amount. Here the β -regression coefficients may be linear or quadratic functions of A . Piepel and Cornell (14) show that this type of polynomial modeling is satisfactory for the hormone blending experimental data of Claringbold (16). For more complex sigmoidal-shaped dose-response surfaces, Minto *et al.* (2) and White *et al.* (3) propose models that generalize the single-drug Hill model to a multiple-drug mixture-amount model.

Typical mixture-amount experimental designs (for two compounds) are lower triangular in nature. This is because the locus of points, $d_1 + d_2 = A$, is a line with a (45 degree angle) slope of -1. Use of several different levels for A results in the lower triangular experimental design as shown in Figure 2. Mixture-amount designs for three or more compounds can be found in Cornell (12).

In a mixture amount experiment, an important class of plots are mixture blending profiles. For a fixed total dose amount (e.g. micromolar), A , of two drug substances, one

can plot the response, y , (or an estimated mean response, $m(x, A, \hat{\beta})$, where $\hat{\beta}$ is an estimate of β) versus x_1 , say.

Such a plot shows how the changing proportion of drug 1 affects the response at a fixed total amount, A . Of course, several such plots can be made for varying amounts, A , to obtain an overall perspective on how drugs 1 and 2 combine to produce responses. See Figures 3A and 3B as an example. Here the nonlinear blending plots can be thought of as “slices” through the response surface along the line given by $d_1 + d_2 = A$ for various amounts, A .

Figures 3A and 3B show blending synergy for the total-dose amount, A , as the proportion of drug 1 is changed from 0 to 1. Here, Figures 3A and 3B correspond to hypothetical inhibition (smaller response is better) experiments. Figure 3A shows a weak form of synergy as the response at 50% of drug 1 is less than the average of the single drug responses, but the best response is still at 0% of drug 1. Figure 3B shows a stronger form of synergy as there exist mixture blends which provide better responses than either drug 1 and 2 alone for a total amount of drug substance, A . We denote Figure 3A an example of “weak nonlinear blending” and Figure 3B as “strong nonlinear blending”. Strong nonlinear blending profiles show experimenters at what total amounts the drug substances should be blended for *improved* efficacy over drugs 1 and 2 alone at the same total dose amount, A . Figures 3A and 3B are for inhibition (i.e. small-the-better) dose-response relationships. For an example involving larger-the-better dose-response relationships, see Peterson and Novick (4).

In addition to a plot as in Figure 3B, it is also possible to show nonlinear blending plots from a dose response curve perspective. Consider the hypothetical dose response curves in Figure 4. Here the gray and black curves represent the single drug agents, while the five red curves represent dose response profiles for drug combinations at five different fixed dose ratios. In Figure 4

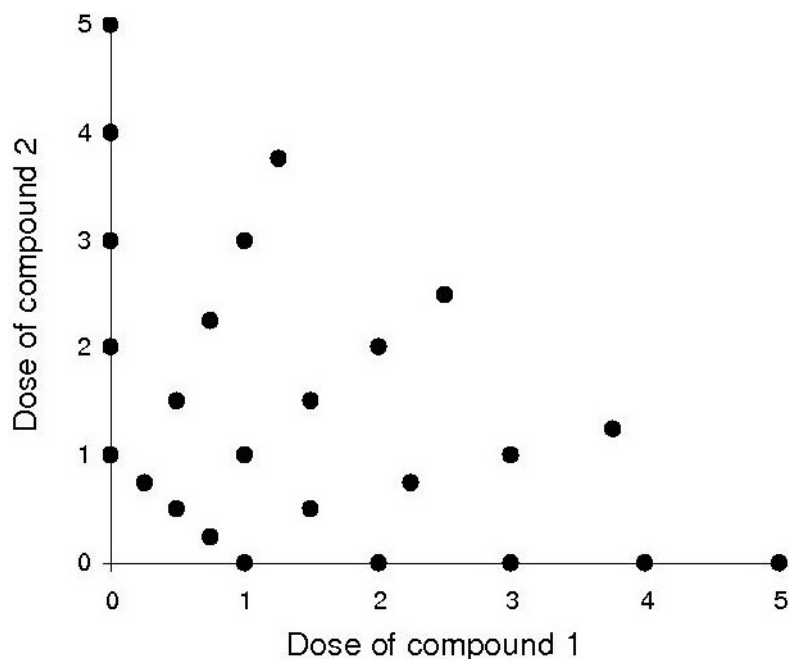


Figure 2. An example of an (unconstrained) mixture-amount experiment layout. Each black point represents an experimental run for a given blend of compounds 1 and 2. Each linear diagonal of points (with slope of -1) corresponds to a fixed total dose amount of compound, with total doses ranging from 1 to 5.

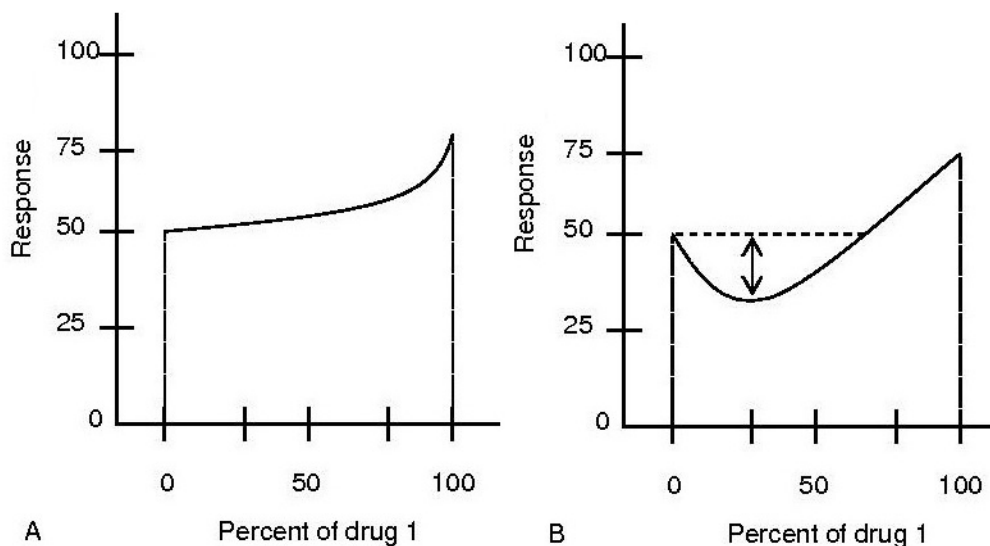


Figure 3. Examples of weak and strong nonlinear blending for hypothetical inhibition (smaller response is better) experiments.

it is clear, that at each fixed total dose level, strong nonlinear blending is present.

Unlike Loewe synergy, the concept of nonlinear blending (NLB) can be applied to any combination drug response surface. Varying relative potency, partial inhibitors, potentiation, and coalism pose no problem at all. Hence NLB offers a general approach to synergy that is needed for the wide variety of response surfaces that could occur with combination drug studies. For each total dose

amount, NLB profiles can be used to quantify synergy directly in the units of response. As seen in Figure 3B, the amount of improvement (over the best single agent) obtained by a 25% blend of drug 1 at total dose *A* is estimated to be about 15 percentage points of response. For an example NLB plot for three-drug combinations, see Peterson and Novick (4).

There is an intimate connection between isobolograms, the Berenbaum index, NLB, and efficacy &

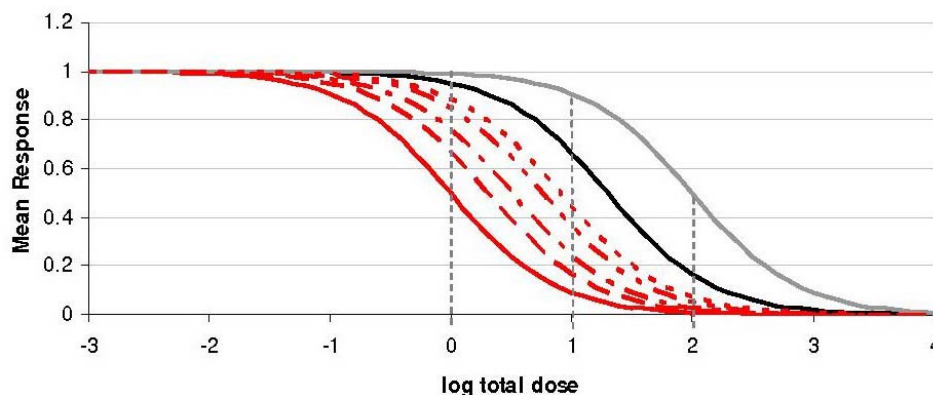


Figure 4. Example of strong nonlinear blending from a dose response curve perspective. The black and gray lines correspond to the single agent dose response curves. Here each red line represents a dose response curve corresponding to a different fixed-dose-ratio drug combination. The dashed vertical lines are reference lines to compare mean response values at specific total dose levels.

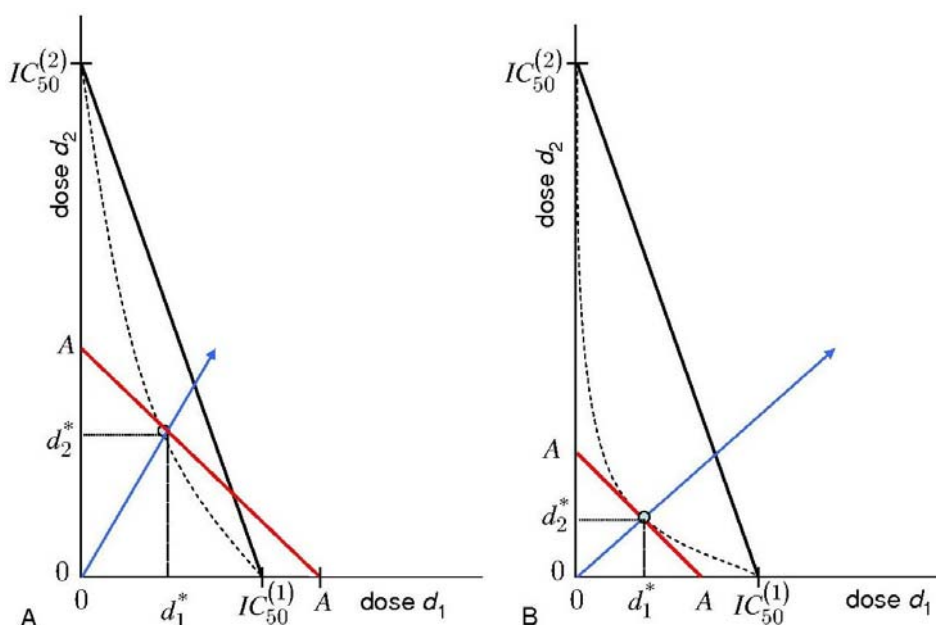


Figure 5. Loewe synergy with a highly potent and low potent drug. Figure 5B shows sufficiently strong Loewe synergy to have strong nonlinear blending. Each dotted line represents an isobologram contour with a 50% response.

potency of drug combinations. Consider the hypothetical example in Figures 5A and 5B. Suppose, for the sake of comparison, that for both of these figures the dose response curves for drugs 1 and 2 have the same shape on the log scale so that Loewe additivity and synergy are well defined. In Figure 5A we see that the 50% isobologram (the dotted line) shows Loewe synergy. Now consider any constant-dose-ratio ray intersecting the isobologram (such as the ray in Figure 5A). One can imagine a dose response curve along this ray, where the “dose” is a mixture-amount of drugs 1 and 2. All drug combinations on this ray have the same dose ratio. Next consider the intersecting point where the ray intersects the 50% isobologram. Suppose that at this point, (d_1^*, d_2^*) , the total dose amount, $d_1^* + d_2^*$,

equals A . Then of course, the line, $d_1 + d_2 = A$, will intersect the points (d_1^*, d_2^*) , $(A, 0)$, and $(0, A)$.

From Figure 5A, one can see that the (d_1^*, d_2^*) combination represents an IC_{50} along the ray that is larger than the IC_{50} for drug 1, despite the fact that we have Loewe synergy. In fact for this particular isobologram it is the case that for any dose combination on the 50% isobologram, the IC_{50} for any intersecting ray is larger than the IC_{50} for drug 1. Granted, the bowed-in isobologram in Figure 5A shows some kind of positive drug interaction but this type of drug synergy is in a sense

rather weak since adding drug 2 appears to dilute drug 1, resulting in a less potent drug combination.

In Figure 5B, one can see that the Loewe synergy is strong enough, so that for some combinations, the IC_{50} along the corresponding ray is smaller than both the IC_{50} 's for drugs 1 and 2 alone. Although, some other points on the 50% isobologram in Figure 5B still correspond to a ray with an IC_{50} larger than that for drug 1. However, as one can see from Figure 5B (for increasing dose-response surfaces) if strong NLB exists at the point (d_1^*, d_2^*) , then the response at (d_1^*, d_2^*) will be larger than the responses corresponding to single compounds at $d_1 = A$ and $d_2 = A$. Hence the IC_{50} 's for the single compounds will both be larger than that for the combination along the ray intersecting (d_1^*, d_2^*) . So, for monotone increasing (or decreasing) dose-response surfaces, strong NLB not only establishes a "synergy of efficacy" along a path of fixed total dose, but it also establishes to a "synergy of potency" along a fixed-dose-ratio ray. The equivalency of "strong NLB" and a "synergy of potency" along a fixed-dose-ratio ray is important as many preclinical and clinical studies employ fixed-dose-ratio experiments (4).

2.3. A dose reduction profile approach to compound blending

An important aspect of combining two anticancer agents is to find a pair that have different modes of toxicity so that lower doses of each one can be used to get efficacy that is as good as or better than either of the single agents alone (19). The existence of strong NLB provides a large degree of such relative dose reduction. Suppose that the dose points (d_1, d_2) , $(D_1, 0)$, $(0, D_2)$ are all on the same isobole contour, where D_i is the dose of drug i alone ($i=1,2$) that gives the same response as the combination dose (d_1, d_2) . It can be shown that if strong NLB exists for the combination (d_1, d_2) then d_1 / D_1 can be at most $d_1 / (d_1 + d_2)$ and d_2 / D_2 can be at most $d_2 / (d_1 + d_2)$. Of course, even if D_1 or D_2 do not exist for a given isobole contour (as with partial inhibitors), strong NLB may still exist.

However, even if strong NLB does not exist, some dose reduction potential may still exist for a combination even in situations of mild antagonism. If two compounds at combination dose (d_1, d_2) exhibit "excess over highest single agent" (20), then $f(d_1, d_2) > \max\{f(d_1, 0), f(0, d_2)\}$, where f is the mean dose response function. If one is screening combination pairs for dose reduction potential, testing for "excess over highest single agent" (EOHSA) is useful as EOHSA is equivalent to $\max\{d_1 / D_1, d_2 / D_2\} < 1$ for monotonically decreasing (increasing) dose response surfaces. In

addition, to testing for EOHSA, it can be helpful to create a plot of $\eta = d_1 / D_1$ vs. $p_1 = d_1 / (d_1 + d_2)$ to see how (as one moves along an isobole contour) changing the proportion of drug 1 affects η (the ratio of drug 1 in the combination, d_1 , to the dose of drug 1 alone, D_1). Likewise, one can make a plot of $r_2 = d_2 / D_2$ vs. p_1 to observe the affect on the ratio of drug 2 in the combination to the dose of drug 2 alone. In fact, it may be best to combine these plots into an overlay plot for a specific isobologram. For several isobolograms, these overlay plots can be made into a trellised plot for better overall visualization across dose response levels. I call such plots "dose reduction profile" (DRP) plots. Such plots can show the relative dose reduction profiles for various blends at a given level of efficacy (given by the isobole). Of course, if there is sufficient antagonism, the η or r_2 ratios may exceed 1 for some blends. DRP plots are shown below in Figures 18 and 19 for the low folic acid and high folic acid experiments, respectively. The idea of examining the ratios involving d_1 and D_1 (or d_2 and D_2) is originally due to Chou and Chou (21); see also Chou (22), although Chou's plotting was done differently.

For a large sample experiments, if one has a smooth, parametric response surface model, one can use the delta method (23, pp486-500) to compute confidence intervals or p -values associated with the dose reduction ratios, η and r_2 . In order to do this one must express η and r_2 as functions of the model parameters, the mean isobole response, and the proportion of one of the two compounds, e.g. p_{TMQ} . An example of this will be given in section 5.

In addition, for prespecified relative dose reduction levels (e.g. $\eta = \eta_0$ and $r_2 = r_{20}$), a specified isobole, and a given combination, one can test

$$H_0 : \eta \geq \eta_0 \text{ or } r_2 \geq r_{20} \text{ vs. } H_1 : \eta < \eta_0 \text{ and } r_2 < r_{20}$$

using the min test (24, Silvapulle and Sen, 2005, p235-239 and pp422-423). Adjustments for multiplicity (across isobole levels and/or combinations) can be done using the Bonferroni approach or the more efficient Simes-Hommel p -value adjustment approach found in Westfall *et al.* (25).

3. RESPONSE SURFACE MODELING

3.1. The molar-unit Minto-White model

Minto *et al.* (2) and White *et al.* (3) have proposed similar hierarchical logistic model approaches to modeling two or more drugs in combination. Their approaches involve the clever idea of fitting logistic dose-response curves along rays of constant dose ratio. All of these curves are then linked together using polynomial models that are functions of the proportions of each drug. Each function models one of the three logistic

regression model parameters ([inflection point] $\log IC_{50}$, Hill slope, and control [left] asymptote value) as a function of the proportions of drugs in the combination at each point of the dose-response surface. The class of polynomial models proposed by Minto *et al.* (2) and White *et al.* (3) are mixture experiment models, although any empirical model form (e.g. parametrically nonlinear model) can be used. Hence the Minto-White (MW) dose-response model is a function of the total dose of the drug combination and the proportions making up that combination. Here, the dose of each drug is measured in units of the IC_{50} of each drug. Hence, the proportions and total dose are also derived using these units.

In this article, I employ a modified version of the Minto-White model, whereby I work in molar units rather than IC_{50} units. This provides a more natural model that can be used even if one or more of the drugs does not possess an IC_{50} . In this article I do not employ a formal mixture experiment model for the three logistic model parameters. This is because with only two drugs it is simpler to employ polynomial functions of the percent of one of the compounds. In this article I chose TMQ. The molar-unit Minto-White (mMW) model has the form

$$f(p_{TMQ}, A) = \begin{cases} B(p_{TMQ}) + \frac{(Econ - B(p_{TMQ}))}{1 + 10^{-m(p_{TMQ})[\log_{10} A - \log_{10} IC_{50}(p_{TMQ})]}} & \text{if } A > 0, \\ Econ & \text{if } A = 0 \end{cases}$$

where p_{TMQ} is the proportion of TMQ and A is the total amount for the drug combination. Here, $B(p_{TMQ})$ is the extrapolated background (asymptote) parameter value corresponding to p_{TMQ} , $m(p_{TMQ})$ is the Hill slope corresponding to p_{TMQ} , and $\log_{10} IC_{50}(p_{TMQ})$ is the logarithm (base 10) of the (inflection-point) IC_{50} as a function of p_{TMQ} . The $Econ$ parameter is the control (left) asymptote. Note that it is not a function of p_{TMQ} because $Econ$ stands for "effect control". Hence it is the mean response associated with no amount of either compound.

The most challenging part of the constructing a MW or mMW model is finding good models for the $B(p_{TMQ})$, $m(p_{TMQ})$, and $\log_{10} IC_{50}(p_{TMQ})$ parameters. It is helpful that the two data sets discussed in this article came from experimental designs where a substantial number of fixed-dose-ratio rays were employed. As such, revealing

plots of the $B(p_{TMQ})$, $m(p_{TMQ})$, and $\log_{10} IC_{50}(p_{TMQ})$ estimates vs. p_{TMQ} can be made.

3.2. Low folic acid experiment

The low folic acid experimental layout employed 13 distinct rays of constant dose ratio. Two of these rays were for TMQ and AG2034 alone, respectively. A four-parameter Hill model was fit to each ray and estimates of B , m , and $\log_{10} IC_{50}$ parameters were obtained for each ray. These estimates were then plotted against their respective p_{TMQ} values to obtain the plots in Figures 6A, 6B, and 6C.

The chosen forms for the $B(p_{TMQ})$, $m(p_{TMQ})$, and $\log_{10} IC_{50}(p_{TMQ})$ hierarchical functions are as follows. The background function, $B(p_{TMQ})$, was chosen to be a constant, B . (Initially, $B(p_{TMQ})$ was chosen to have a quadratic form but neither the linear nor quadratic hierarchical parameters were statistically significant at the 5% level and the AIC model selection statistic (26, p60) preferred the constant form for $B(p_{TMQ})$.) The Hill slope function, $m(p_{TMQ})$, was chosen to have a cubic polynomial form, while the $\log_{10} IC_{50}(p_{TMQ})$ function was chose to have a linear form. To help reduce correlation among the hierarchical parameters in the cubic form for the Hill slope, $m(p_{TMQ})$ was expressed as a cubic polynomial in $(p_{TMQ} - 0.5)$. To accommodate heteroscedasticity in the residuals, a 'power of the mean' function was used to model the residual variance. Here,

$$Var(e) = \sigma^2 f(p_{TMQ}, A)^\phi,$$

where e is the residual error. The mMW model was fit using PROC NL MIXED in SAS[®] v9.1.3.

Because a 'power of the mean' function was used to model the residual variance, a standardized residual analysis was done to check for model adequacy. The estimated standardized residual here is defined to be ε , where ε is defined as \hat{e} divided by the square root of the estimated variance of e . Here, \hat{e} is the estimated residual. An initial residual plot of ' ε vs. predicted values' indicated that four observations have residuals more than four standard deviations from zero. As such, these four observations were deleted as outliers.

Table 1. Parameter estimates and standard errors for the (molar-unit) Minto-White model (low folic acid experiment)

| Logistic parameter form | Hierarchical parameters | Max. likelihood estimate | Asymptotic standard error of the estimate |
|---------------------------------|-------------------------|--------------------------|---|
| $B(p_1)$ =constant | | $B=0.1312$ | 0.001739 |
| $m(p_1)$ =cubic | intercept | $mi=-3.7947$ | 0.1855 |
| | linear term | $ml=6.3580$ | 0.6388 |
| | quadratic term | $msq=7.4042$ | 0.8237 |
| | cubic term | $mcu=-27.3468$ | 2.9223 |
| $\log_{10}IC_{50}(p_1)$ =linear | intercept | $IICi=-2.7163$ | 0.008662 |
| | linear term | $IICl=-0.3820$ | 0.02181 |
| Econ | | $Econ=1.1792$ | 0.00998 |
| Power of the mean | baseline variance | $\sigma^2 = 0.02533$ | 0.001795 |
| | exponent | $\phi = 1.7189$ | 0.05966 |

The parameter estimates (with outliers deleted) are given in Table 1 below. The R^2 for this model is 94.8%.

A standardized residual plot corresponding to the model specified by Table 1 is given in Figure 7A. Here, one can see that the residuals appear quite random, although there is still a slight bulging associated with the intermediate predicted values. A histogram of the standardized residuals is given in Figure 7B. As one can see, these residuals appear to have approximately a normal distribution, with slightly heavier tails than a normal distribution.

A 3D plot of the dose response surface is given in Figure 8. This response surface is presented on the log scale using $\log_{10}TMQ$ and $\log_{10}AG2034$ as the predictor variables. The surface is normalized by dividing all predicted mean values by the estimate for $Econ$. An isobologram plot of the normalized dose-response surface is shown in Figure 9, with isoboles for 0.9 to 0.2. An isobole of 0.1 is not shown because the $B(p_{TMQ})$ values are greater than 0.1 for all p_{TMQ} proportions. (Also, note that all values of B in Figure 6A are greater than 0.1.)

3.3. High folic acid experiment

The high folic acid experimental layout also employed 13 distinct rays of constant dose ratio. Two of these rays were for TMQ and AG2034 alone, respectively. A four-parameter Hill model was fit to each ray and estimates of B , m , and $\log_{10}IC_{50}$ parameters were obtained for each ray. These estimates were then plotted against their respective p_{TMQ} values to obtain the plots in Figures 10A, 10B, and 10C.

For the high folic acid experiment, it appears that some of the three logistic model parameters vary most naturally on the log scale relative to the proportion of TMQ in the drug combination. The log transformation used is $\log_{10}(p_{TMQ}+0.0001)+2$, where p_{TMQ} is the proportion of TMQ in the combination. The value of 0.0001 is an offset so that the transformation is bounded for $p_{TMQ}=0$. The addition of 2 is to approximately center the log-transformed values around zero to reduce the correlation among some of the hierarchical parameter estimates in the polynomial functions of the transformed p_{TMQ} . The selected forms for

the $B(p_{TMQ})$, $m(p_{TMQ})$, and $\log_{10}IC_{50}(p_{TMQ})$ are as follows. The B -parameter function was chosen as linear in the transformed p_{TMQ} proportion. The Hill slope function, $m(p_{TMQ})$, was modeled as linear in the transformed p_{TMQ} proportion. The $\log_{10}IC_{50}(p_{TMQ})$ parameter was modeled as quadratic in the transformed p_{TMQ} proportion.

As with the low folic acid experiment, a 'power of the mean' model was also used to model error heteroscedascity. An initial residual plot of ' ε vs. predicted values' indicated that two observations have residuals more than four standard deviations from zero. As such, these two observations were deleted as outliers.

The parameter estimates (with outliers deleted) are given in Table 2. The R^2 for this model is 94.4%. As for the low folic acid experiment, the residuals for the high folic acid experiment appear to be reasonably random and normally distributed. See Figures 11A and 11B.

A 3D plot of the dose response surface is given in Figure 12. This response surface is presented on the log scale using $\log_{10}TMQ$ and $\log_{10}AG2034$ as the predictor variables. The surface is normalized by dividing all predicted mean values by the estimate for $Econ$. An isobologram plot of the normalized dose-response surface is shown in Figure 13, with isoboles for 0.9 to 0.2. An isobole of 0.1 is not shown because the $B(p_{TMQ})$ values are greater than 0.1 for all p_{TMQ} proportions. (Also, note that all values of B in Figure 10A are greater than 0.1.)

4. NONLINEAR BLENDING ANALYSIS

4.1. Strong nonlinear blending

The NLB plots in Figures 15 and 17 show how the change in the fraction of TMQ affects the mean response. Such plots need to be made for a variety of total dose values, as the nature of NLB curves may change for different total dose levels. In addition, further insight may be obtained by also viewing from an alternative dose response perspective. This perspective is to create plots of a dose response curve for a number of fixed-dose-ratio rays. Such (alternate nonlinear blending) plots can be distilled

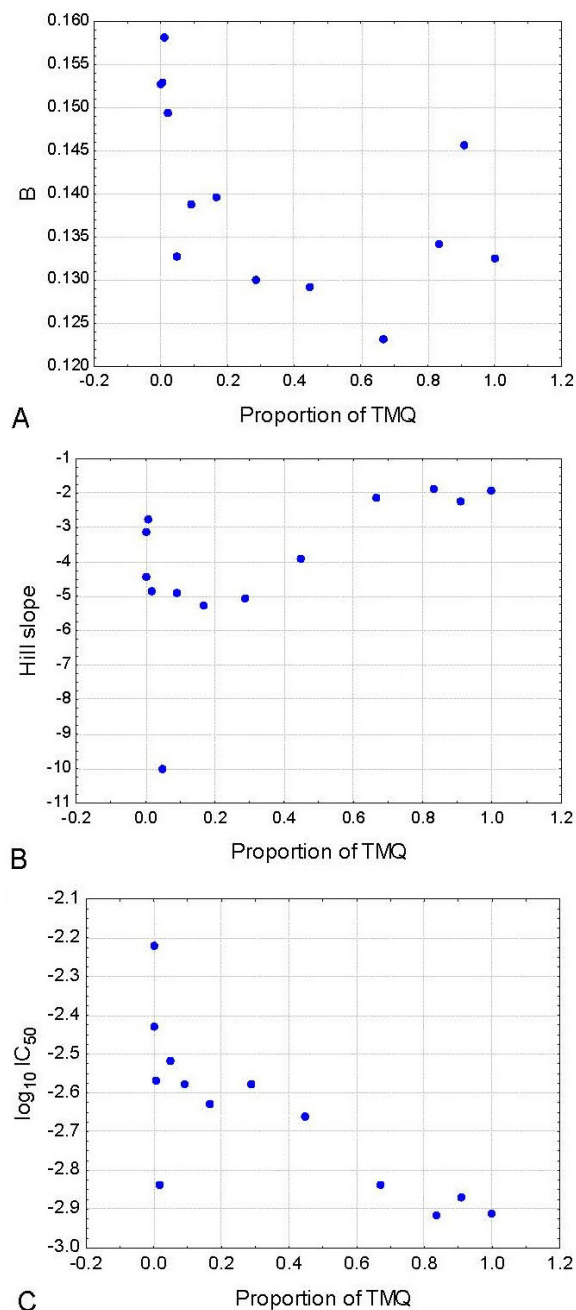


Figure 6. Plots of logistic model parameter estimates (B, Hill slope, & $\log_{10}IC_{50}$) vs. the proportion of TMQ (low folic acid experiment).

from the dose response surface based upon the mMW model, by "slicing" the response surface along these rays. As a reference, each combination-drug dose-response curve can be plotted in an overlay plot with the two single-drug dose-response curves. Such plots (shown in Figures 14 and 16) provide a view of how the mean response changes with the total amount of drug in combination. One should make such overlay plots for various proportions of one of the drugs. These graphical analyses are illustrated in the two

subsections below for the low and high folic acid experiments, respectively.

4.2. Low folic acid experiment

Based upon the mMW model in section 3.2, nine dose-response NLB plots are shown in Figure 14 corresponding to the proportions of TMQ from 0.1 to 0.9 by 0.1. The dose response curve corresponding to the combination along the ray is in red. The reference curves corresponding to TMQ alone and AG2034 alone are given by the curves in gray and black, respectively. From Figure 14, one can see that variations in the fraction of TMQ change the slope of the combination-drug dose-response curves, but real no improvement in efficacy or potency appears to exist. It is evident that TMQ alone provides the best dose response curve.

NLB can also be assessed for various fixed total doses as in Figure 15. Nine total doses from 0.0005 micromolar to 0.005 micromolar (equally spaced on the log dose scale) were chosen based upon the contour range in Figure 9. From Figure 15, one can also see that there is virtually nothing to be gained from an efficacy or potency perspective by blending AG2034 with TMQ. For the total dose levels of 0.0037 micromolar and 0.005 micromolar, some drug blends appear to do about as well as 100% TMQ, but really no better. Hence, it appears that the addition of AG2034 tends to, more or less, dilute the TMQ. This is because the positive interaction of TMQ and AG2034 is not sufficiently strong enough to overcome the diluting effect of replacing some of the TMQ molecules with AG2034 molecules, at the total doses studied in this experiment.

For each of the nine total dose levels in Figure 15, a confidence set of TMQ proportions associated with the minimum mean response can be computed using the method of Peterson *et al.* (27). The confidence sets are given in Table 3. Note that some of these confidence sets are single points or the union of disjoint sets, as for example, total doses 0.0012 micromolar and 0.0028 micromolar, respectively. A confidence set consisting of a single point is possible for minimizations (or maximizations) for a constrained parameter, such as a proportion which must be in the interval $[0, 1]$. A confidence set that does not contain the boundary points 0 or 1 means that a minimum mean response exists only for a mixture of the two drugs, thereby implying *strong* NLB in a statistically significant way. Likewise, a confidence set containing either boundary point, 0 or 1, indicates that strong NLB may not exist at the total dose amount in question. The nine confidence sets were adjusted using the Bonferroni criterion to provide a simultaneous coverage rate of at least 95%. As one can see from Table 3, strong NLB was only evident (in a statistically significant way) for the lowest dose examined, 0.0005 μM .

From Table 3 one can also see, from an *in-vitro* efficacy standpoint, that there is little or no statistical evidence to blend AG2034 with TMQ. Of the nine total doses, only the lowest total dose, 0.0005 micromolar, has a confidence set for minimizing TMQ proportions that does not contain 0 or 1. However, even the upper bound of this confidence set is very close to 1.

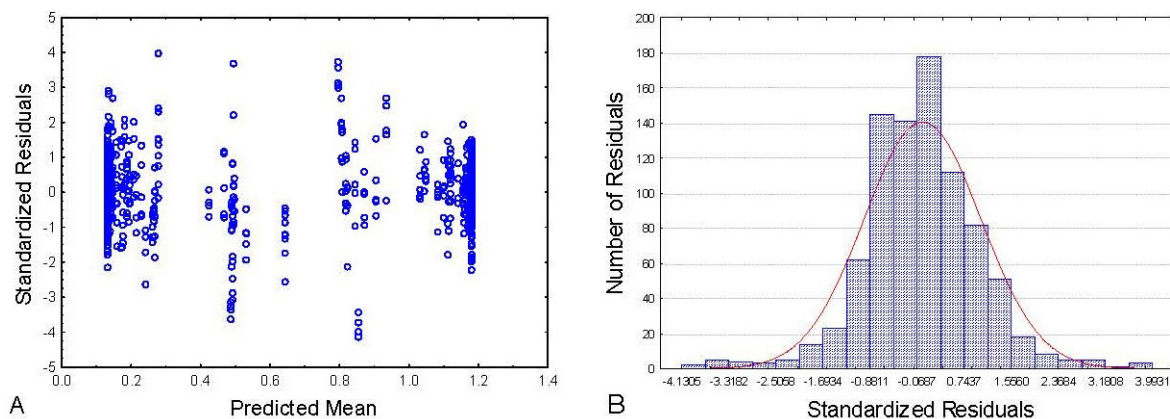


Figure 7. Plot of standardized residuals (A.) and histogram of standardized residuals (B.) for (molar-unit) Minto-White model (low folic acid experiment).

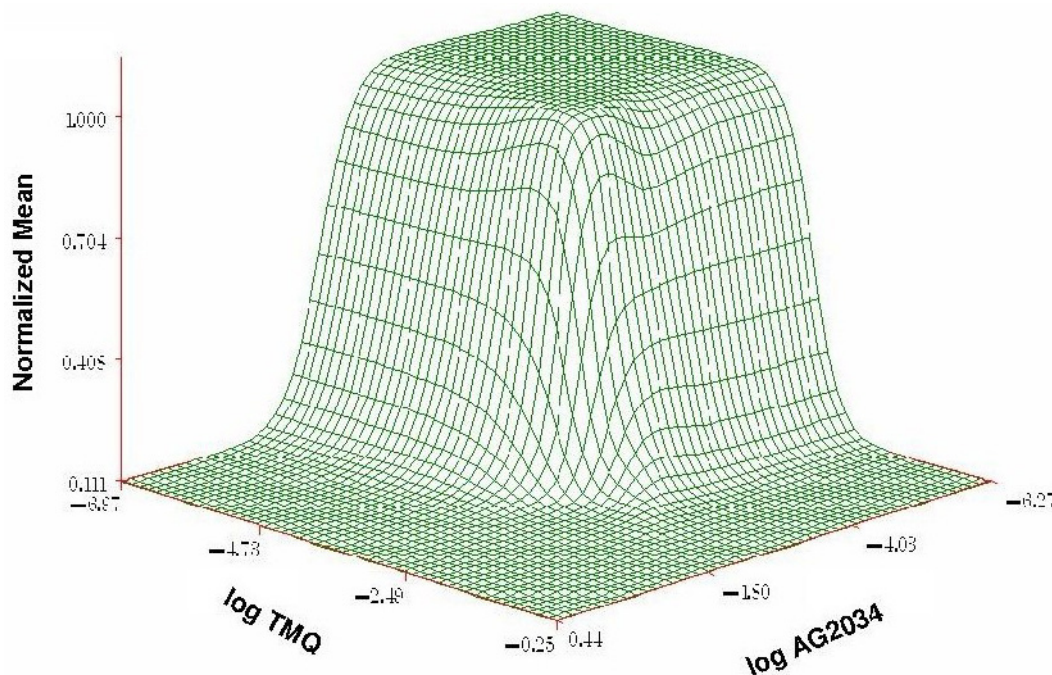


Figure 8. Normalized mean dose response surface for combinations of TMQ and AG2034 (low folic acid experiment).

4.3. High folic acid experiment

Based upon the mMW model in section 3.3, nine dose-response NLB plots are shown in Figure 16 corresponding to the proportions of TMQ from 0.1 to 0.9 by 0.1. The dose response curve corresponding to the combination along the ray is in red. The reference curves corresponding to TMQ alone and AG2034 alone are given by the curves in gray and black, respectively. One can see from Figure 16, that when TMQ is only 10% of the combination, the dose response curve along that fixed-dose-ratio ray is already close to the one for 100% TMQ. In addition, one can see that the dose response curve for TMQ alone is superior for TMQ proportions between 0.1 and 0.6; for proportions 0.7 to 0.9 the

gray and red curves virtually overlap. From Figure 16, it is evident that TMQ alone provides the best dose response curve.

The NLB plots in Figure 17 show that blending in TMQ decreases the mean response for all of the nine dose levels (equally spaced on the log dose scale) from 0.005 micromolar to 0.05 micromolar so that 100% of TMQ is the optimal blend for each total dose level. As with the low folic acid experiment, for the high folic acid experiment, it appears that the addition of AG2034 simply dilutes the TMQ. This is because the (Loewe) "synergistic" interaction of TMQ and AG2034 is not sufficiently strong enough to overcome the diluting effect of replacing some

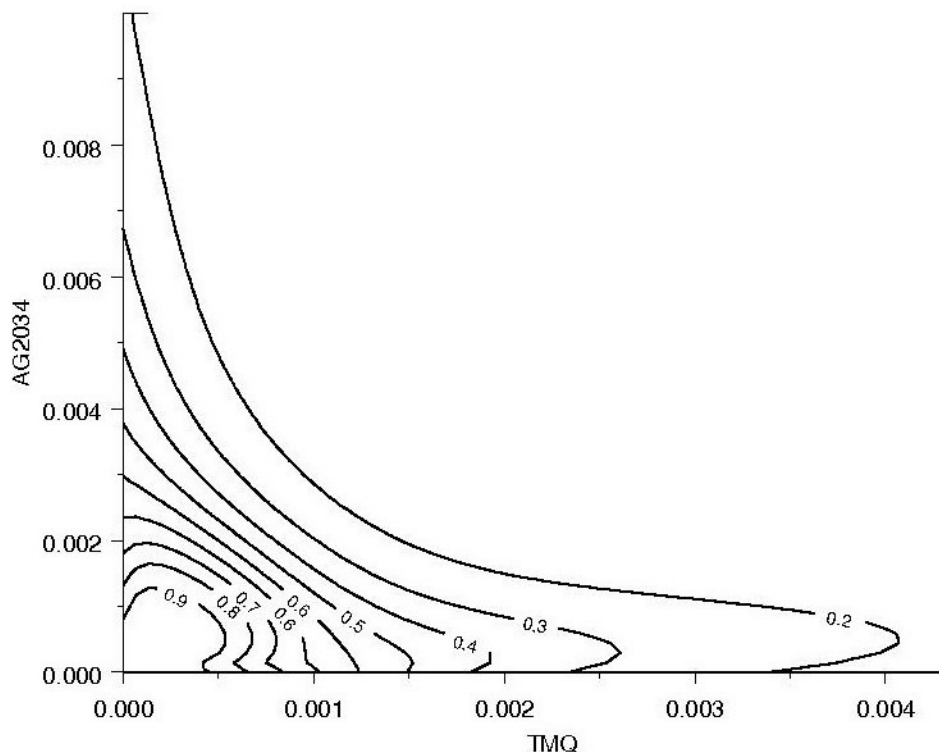


Figure 9. Isobologram contour plot of normalized dose response surface for low folic acid experiment.

of the TMQ molecules with AG2034 molecules, at the total doses studied in this experiment.

Using the approach in Peterson *et al.* (27), one can show in a statistically significant manner that the optimal proportion of TMQ for each of the nine total doses is 100% TMQ. This is done by computing (Bonferroni adjusted) 95% confidence sets for each of the nine total doses. In each case the confidence set was composed of the single point 1. Hence, there is statistically significant evidence that for total dose amounts of 0.005 micromolar to 0.05 micromolar blending in AG2034 only dilutes the efficacy of TMQ. In other words, the AG2034-TMQ Loewe synergy (as shown by the isobologram plot in Figure 13) is not enough to overcome the diluting effect of the less potent compound AG2034.

5. ANALYSIS OF DOSE REDUCTION PROFILES

5.1. Dose reduction profile curves

In viewing the isobles in Figures 9 and 13, one may be able to see, that for some dose combinations, the levels of TMQ and AG2034 are lower than for the respective amounts of TMQ and AG2034 alone on that same isobole. However, making this assessment from viewing the isobolograms is not graphically optimal. For some isoboles in Figure 9 it is difficult to tell if such dose combinations exist. A dose reduction profile (DRP) as described in section 2.3, on the other hand, makes such an assessment immediate. This is because it is a direct overlay plot of respective (combination by single agent) dose ratios

versus the proportion of one of the drugs in the combination.

Also as mentioned in section 2.3, one can make large sample statistical inferences for η_1 and η_2 using the delta method. For the mMW model, $f(p_{TMQ}, A)$, this can be done as follows. Recall that $r_i = d_i / D_i$ ($i=1,2$), where d_1 and d_2 are the doses for the combination where $d_1 + d_2 = A$ and $p_{TMQ} = p_1 = d_1 / (d_1 + d_2)$. (Here, TMQ is denoted by drug 1 and AG2034 by drug 2.) Suppose $y = f(p_{TMQ}, A; \theta) / Econ$, for some (normalized) mean response value, y , where θ is the vector of regression model parameters in the mMW model. Solving the $y = f(p_{TMQ}, A; \theta) / Econ$ equation for A (for $B(p_{TMQ}) / Econ < y < 1$) yields $A = g(p_{TMQ}, y; \theta)$, where $g(p_{TMQ}, y; \theta)$ equals

$$10^{\log_{10} IC_{50}(p_{TMQ})} \left[\frac{(Econ - yEcon)}{(yEcon - B(p_{TMQ}))} \right]^{-1/m(p_{TMQ})}.$$

Note that $A = D_1$ when $p_{TMQ} = 1$ and $A = D_2$ when $p_{TMQ} = 0$. Hence, $D_1 = g(1, y; \theta)$ and $D_2 = g(0, y; \theta)$. Thus D_1 and D_2 can be expressed as functions of y and θ ,

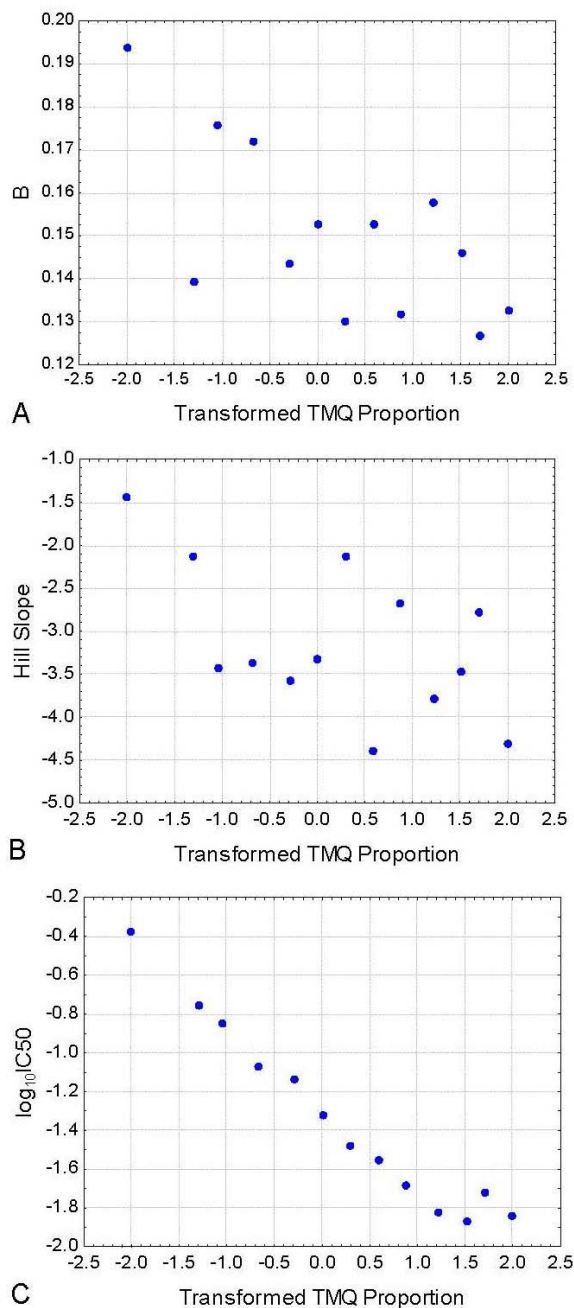


Figure 10. Plots of logistic model parameter estimates (B, Hill slope, & $\log_{10}IC_{50}$) vs. the transformed proportion of TMQ (high folic acid experiment).

if A can be expressed as $g(p_{TMQ}, y; \theta)$. Furthermore, since $d_1 = p_{TMQ}A$ and $d_2 = p_{AG2034}A = (1 - p_{TMQ})A$, we can express d_1 as $p_{TMQ}g(p_{TMQ}, y; \theta)$ and d_2 as $(1 - p_{TMQ})g(p_{TMQ}, y; \theta)$. Hence one can use the delta method to obtain large sample confidence intervals or hypothesis tests about r_1 and r_2 . Note that because r_1 and

r_2 are bounded below by zero, it is better to make (delta method) inferences using $\log r_1$ and $\log r_2$, and then use anti-logs for the final expressions associated with r_1 and r_2 . Confidence intervals and test statistics involving $\log r_1$ and $\log r_2$ (using the delta method) can be easily obtained by PROC NLMIXED using the PREDICT statement.

It may also be possible to construct simultaneous confidence bands about the underlying DRP curves in order to assess their uncertainty in a more complete fashion. However, this is left as a further research problem.

5.2. Low folic acid experiment

From Figure 18 one can see that for all isobole contours, except possibly the ones equal to 0.5 or 0.6, the profiles exceed 1 for certain proportions of TMQ. However, one should also note that, by viewing the DRP plot one can observe that for TMQ proportions around 0.25-0.3 the profiles corresponding to AG2034 and TMQ intersect. It is these intersection points where both drugs in combination can be brought to the same ratio relative to their single drug dose level. Such intersection points can be of interest if the corresponding ratio is small. As can be seen in Figure 18, the profile intersection points are less than 0.5 for the isobole contours 0.2, 0.3, and 0.4. This implies that better dose reduction for both drugs may be possible at higher efficacy levels for this combination of drugs.

Table 4 shows the point estimates and large sample confidence intervals for r_1 and r_2 at $p_{TMQ} = 0.25$ for mean response isobole values from 0.2 to 0.9. These confidence intervals were created as described above in section 5.1. The Bonferroni adjustment was performed across all sixteen confidence intervals to obtain 95% simultaneous confidence intervals. It can be seen from Table 4 that, for isoboles from 0.2 to 0.7, the corresponding r_{TMQ} and r_{AG2034} values are less than one in a statistically significant way.

5.3. High folic acid experiment

For the high folic acid experiment, Figure 19 shows that the profile intersection points correspond to rather low ratios and quite low levels of TMQ for all of the eight isoboles from 0.2 to 0.9. Hence, at a high folic acid level, only small amounts of TMQ are needed to make both dose ratios small.

Table 5 shows that, even when p_{TMQ} is only 1% of the total amount in combination, both dose ratios, r_{TMQ} and r_{AG2034} are noticeably small for all of the mean response isoboles from 0.2 to 0.9.

6. SUMMARY AND PERSPECTIVE

The two data sets obtained from the low and high folic acid experiments are very nice examples of data

Table 2. Parameter estimates and standard errors for the (molar-unit) Minto-White model (high folic acid experiment)

| Logistic parameter form | Hierarchical parameters | Max. likelihood estimate | Asymptotic standard error of the estimate |
|-------------------------------------|-------------------------|--------------------------|---|
| $B(p_1)$ = linear | intercept | $Bi=0.1363$ | 0.002601 |
| | linear term | $Bl=-0.00757$ | 0.002369 |
| $m(p_1)$ = linear | intercept | $mi=-2.2211$ | 0.07203 |
| | linear term | $ml=-0.2342$ | 0.06490 |
| $\log_{10}IC_{50}(p_1)$ = quadratic | intercept | $lICi=-1.3502$ | 0.009128 |
| | linear term | $lICl=-0.4135$ | 0.006733 |
| | quadratic | $lICq=0.06748$ | 0.005010 |
| Econ | | $Econ=1.1562$ | 0.006812 |
| Power of the mean | baseline variance | $\sigma^2 = 0.01586$ | 0.000931 |
| | exponent | $\phi = 1.4295$ | 0.05919 |

Table 3. Simultaneous 95% confidence sets for the minimizing proportion of TMQ for fixed total doses (as given in Figure 15) for the low folic acid experiment

| Total dose (micromolar) | Confidence Set |
|-------------------------|-------------------------|
| 0.0005 | [0.87, 0.97] |
| 0.00067 | [0.88, 1] |
| 0.00089 | [0.90, 1] |
| 0.0012 | {1} |
| 0.0016 | {1} |
| 0.0021 | {1} |
| 0.0028 | [0.51, 0.62] \cup {1} |
| 0.0037 | [0.42, 0.51] \cup {1} |
| 0.005 | [0.38, 0.45] \cup {1} |

Table 4. Point estimates and simultaneous 95% confidence intervals (in parenthesis) for the dose ratios for various isobole levels for the low folic acid experiment. Here, the proportion of TMQ is 0.25

| Isobole | Dose ratios for $p_{TMQ} = 0.25$ | |
|---------|----------------------------------|----------------------|
| | r_{TMQ} | r_{AG2034} |
| 0.2 | 0.29 (0.23, 0.35) | 0.27 (0.23, 0.32) |
| 0.3 | 0.36 (0.31, 0.41) | 0.37 (0.34, 0.41) |
| 0.4 | 0.41 (0.37, 0.45) | 0.46 (0.43, 0.49) |
| 0.5 | 0.46 (0.41, 0.51) | 0.55 (0.53, 0.57) |
| 0.6 | 0.51 (0.45, 0.57) | 0.65 (0.62, 0.68) |
| 0.7 | 0.57 (0.49, 0.66) | 0.77 (0.71, 0.83) |
| 0.8 | 0.65 (0.53, 0.79) | 0.94 (0.84, 1.07) |
| 0.9 | 0.79 (0.60, 1.03) | 1.28 (1.06, 1.55) |

Table 5. Point estimates and simultaneous 95% confidence intervals (in parenthesis) for the dose ratios for various isobole levels for the high folic acid experiment. Here, the proportion of TMQ is 0.01

| Isobole | Dose ratios for $p_{TMQ} = 0.01$ | |
|---------|----------------------------------|--------------------------|
| | r_{TMQ} | r_{AG2034} |
| 0.2 | 0.045 (0.039, 0.053) | 0.054 (0.041, 0.071) |
| 0.3 | 0.041 (0.035, 0.047) | 0.064 (0.052, 0.079) |
| 0.4 | 0.039 (0.034, 0.44) | 0.070 (0.058, 0.84) |
| 0.5 | 0.037 (0.033, 0.042) | 0.075 (0.062, 0.090) |
| 0.6 | 0.036 (0.031, 0.040) | 0.0794 (0.065, 0.097) |
| 0.7 | 0.034 (0.030, 0.039) | 0.084 (0.067, 0.110) |
| 0.8 | 0.033 (0.028, 0.038) | 0.090 (0.069, 0.119) |
| 0.9 | 0.031 (0.026, 0.036) | 0.100 (0.070, 0.142) |

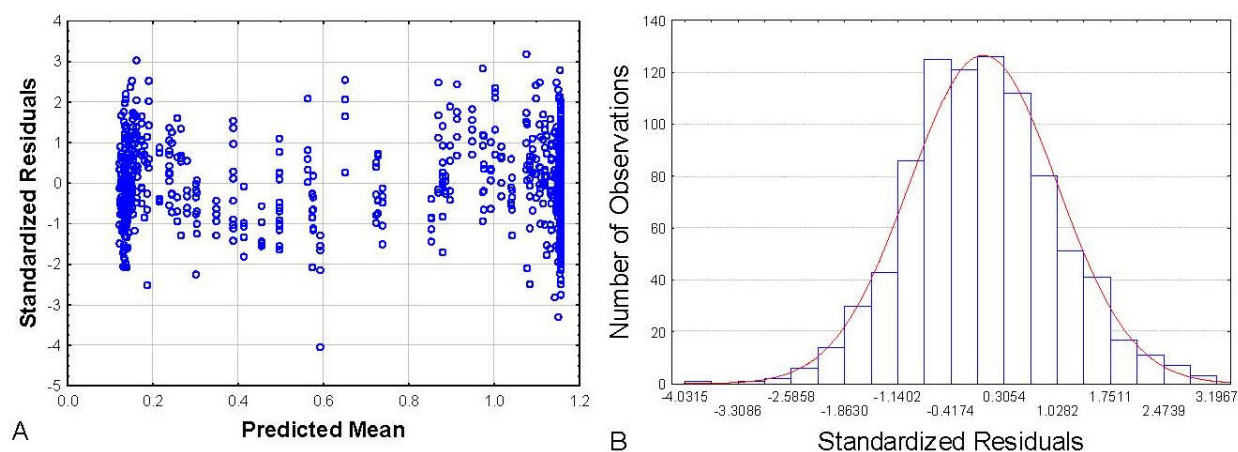


Figure 11. Plot of standardized residuals (A.) and histogram of standardized residuals (B.) for (molar-unit) Minto-White model (high folic acid experiment).

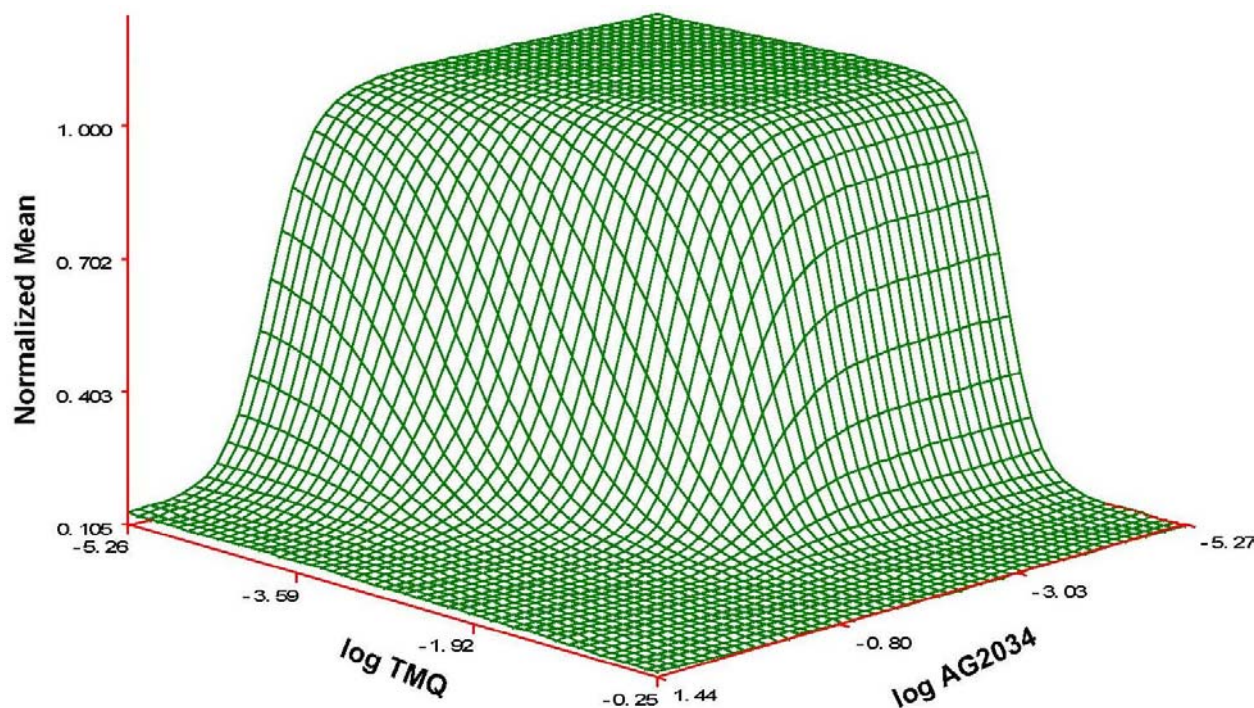


Figure 12. Normalized mean dose response surface for combinations of TMQ and AG2034 (high folic acid experiment).

from carefully planned experiments that do not skimp on information. As such they allow researchers to build good dose-response models for the underlying drug interactions. It is clear that the levels of folic acid affect the interactions of AG2034 and TMQ. At a high level of folic acid, TMQ and AG2034 appear to have a larger interaction effect than for the low folic acid level.

From the perspective of strong NLB, both the low and high folic acid experiments show that, with regard to increased potency or efficacy, little or no synergy is gained by blending in AG2034 with TMQ at any of the total dose levels shown in Figures 15 and 17, respectively.

This is supported for the most part by the confidence set method of Peterson *et al.* (27).

On the other hand, it does appear that the blending of AG2034 and TMQ does offer excellent dose reduction potential for the high level of folic acid. From the DRP plots in Figure 19 one can see that for each of the eight isoboles (from 0.2 to 0.9) blending in only a small amount of TMQ greatly reduces that amount of AG2034 that is required for the same level of response as that of AG2034 alone. For the high folic acid experiment (see Figure 19 and Table 5) there are dose combinations where both dose ratios, r_{TMQ} and r_{AG2034} , are small (e.g. in the

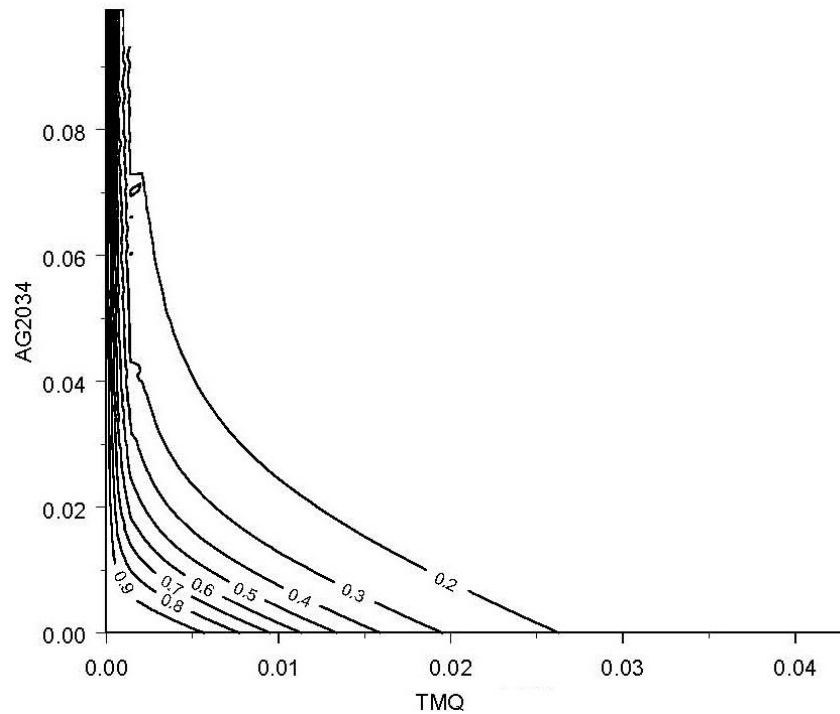


Figure 13. Isobologram contour plot of normalized dose response surface for high folic acid experiment.

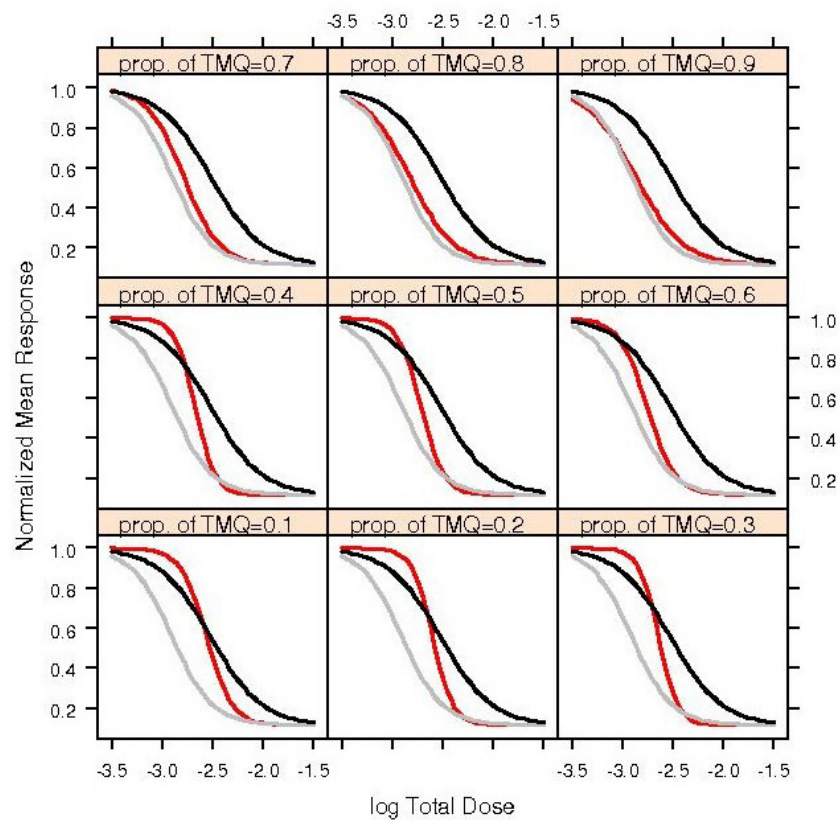


Figure 14. Nonlinear blending plots (dose response perspective) for low folic acid by proportion of TMQ. Key: Black line = AG2034 alone, Gray Line = TMQ alone, Red line= combination.

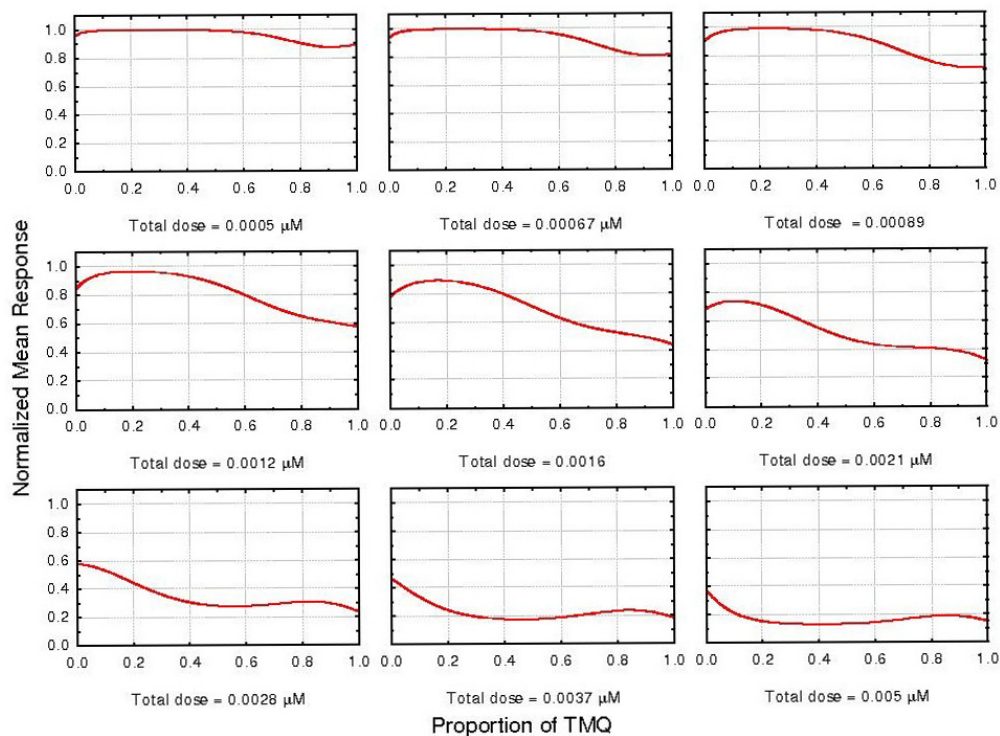


Figure 15. Nonlinear blending plots for low folic acid by total dose.

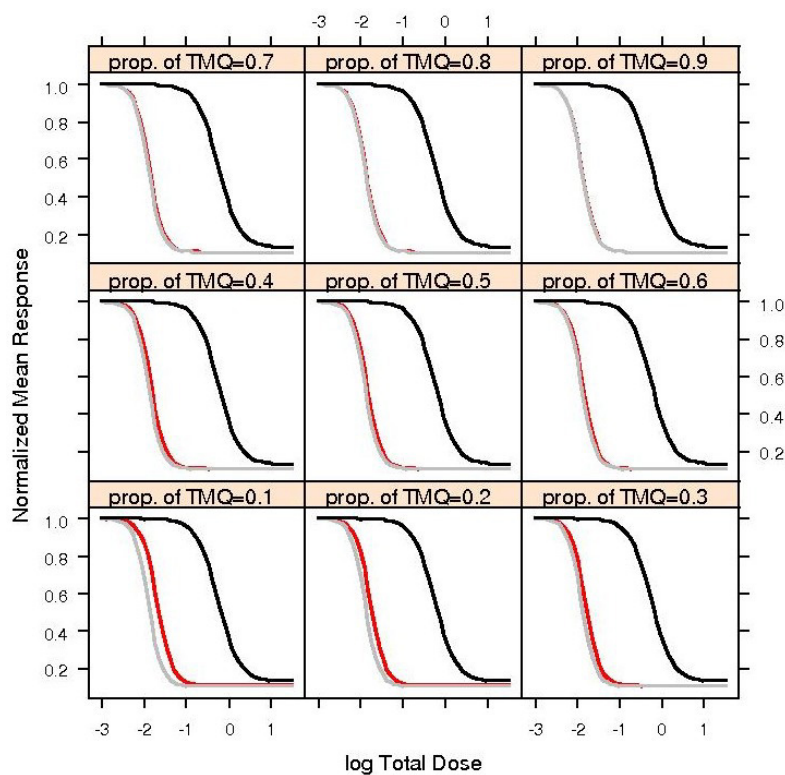


Figure 16. Nonlinear blending plots (dose response perspective) for high folic acid by proportion of TMQ. Key: Black line = AG2034 alone, Gray Line = TMQ alone, Red line= combination. Note that for TMQ proportions of 0.7, 0.8, and 0.9 the red and gray lines virtually overlap.

Synergy concepts of nonlinear blending and dose-reduction profiles

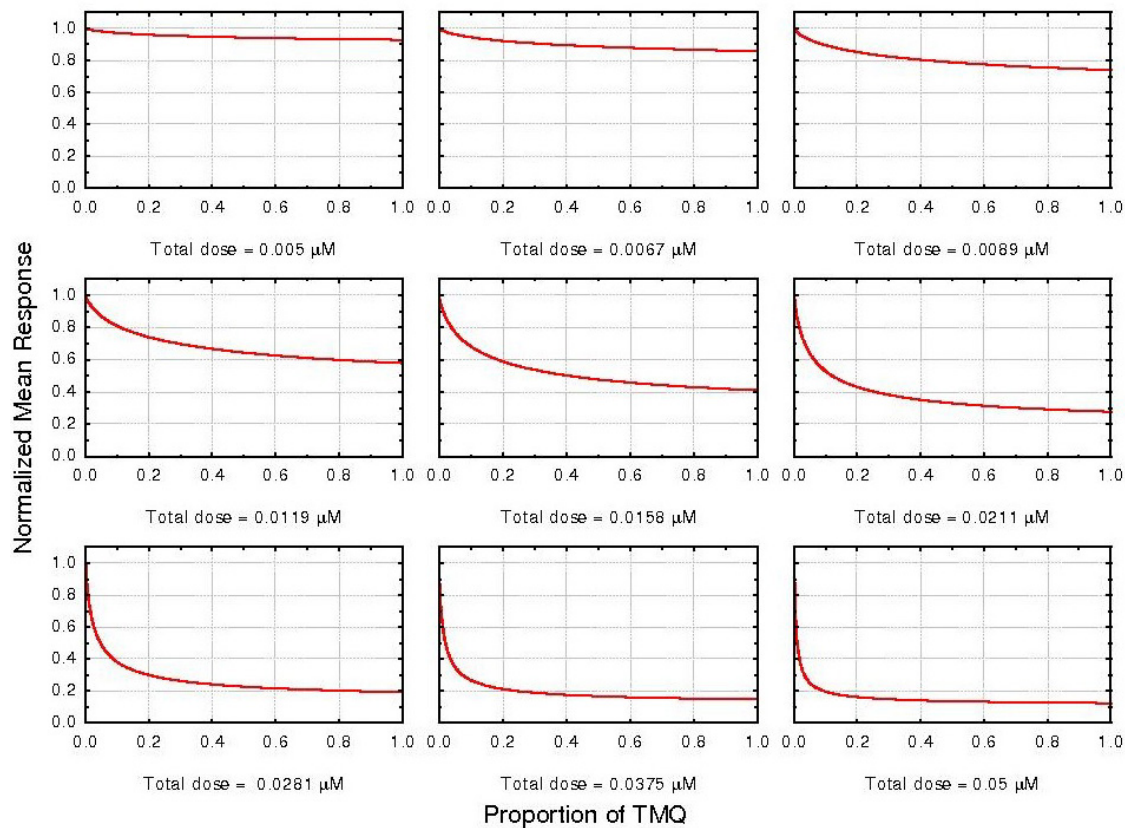


Figure 17. Nonlinear blending plots for high folic acid by total dose.

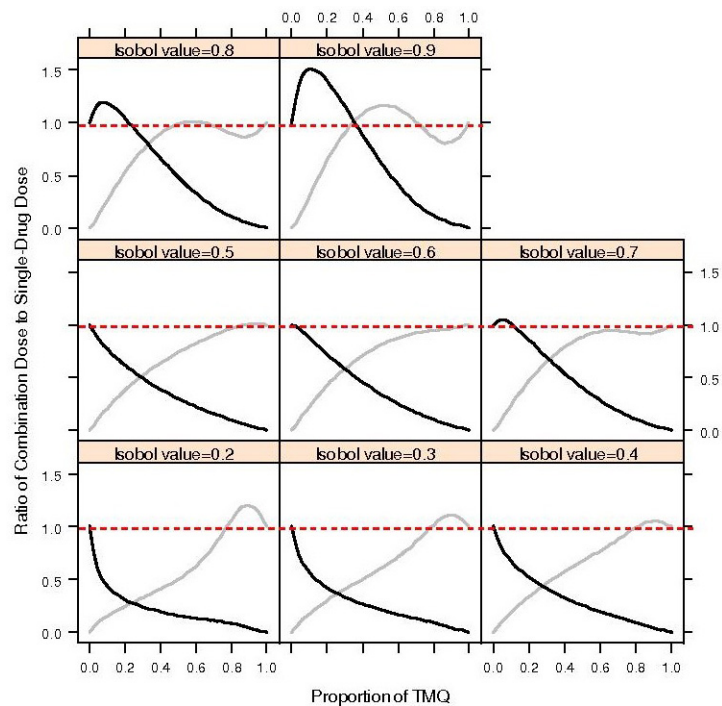


Figure 18. Dose reduction profile plots (low folic acid experiment). The gray line (TMQ) is the ratio $r_{\text{TMQ}} = d_{\text{TMQ}} / D_{\text{TMQ}}$, while the black line (AG2034) is the ratio $r_{\text{AG2034}} = d_{\text{AG2034}} / D_{\text{AG2034}}$. The red dotted line is a reference line for a ratio of one.

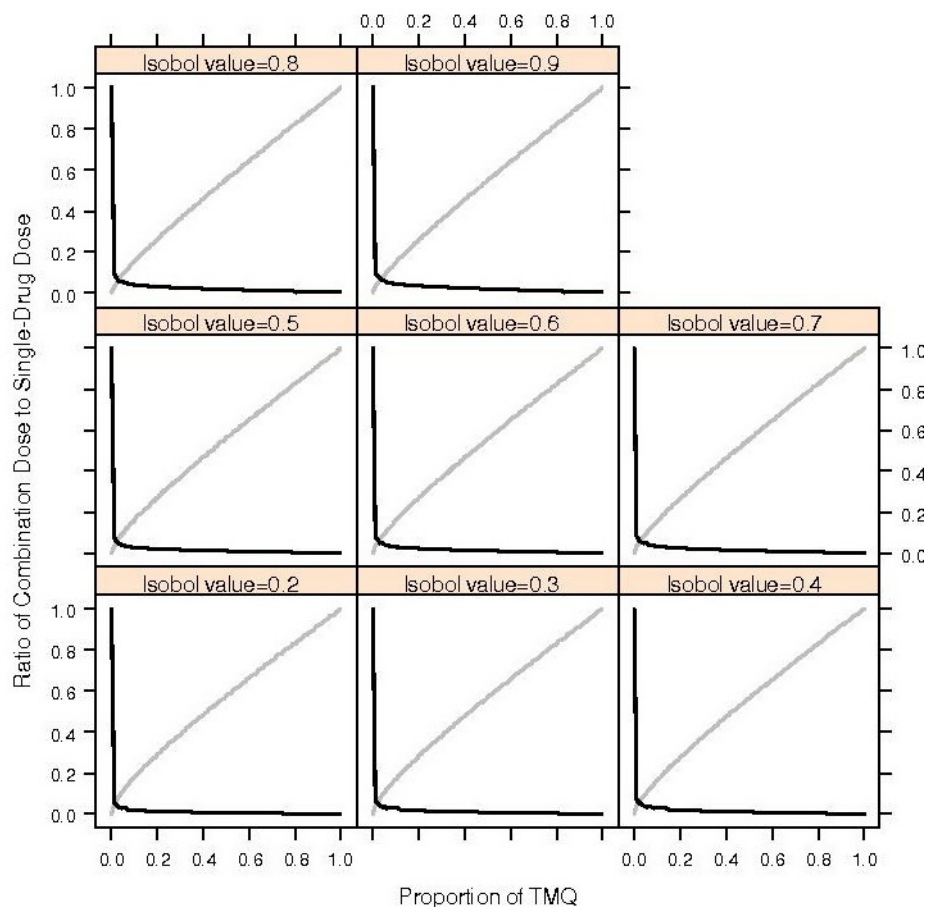


Figure 19. Dose reduction profile plots (high folic acid experiment). The gray line (TMQ) is the ratio $r_{\text{TMQ}} = d_{\text{TMQ}} / D_{\text{TMQ}}$, while the black line (AG2034) is the ratio $r_{\text{AG2034}} = d_{\text{AG2034}} / D_{\text{AG2034}}$.

neighborhood of 0.1 or less). Since the Berenbaum index is $I = r_{\text{TMQ}} + r_{\text{AG2034}}$, it follows that for some dose combinations on various isoboles, I is much less than 1. This would account for the statement of "super *in-vitro* synergy" mentioned in Faessel *et al.* (1). If $I < 1$, then of course both r_{TMQ} and r_{AG2034} are less than 1. However, it is more informative to directly analyze each dose ratio separately.

In conclusion, it is worth pointing out that the concept of strong NLB can be applied to dose-response surfaces even more complex than those shown in these case studies. Unlike Loewe synergy, the concept of nonlinear blending (NLB) can be applied to any combination drug response surface. Varying relative potency, partial inhibitors, potentiation, and coalism pose no problem at all. Hence NLB offers a general approach to synergy that is needed for the wide variety of response surfaces that could occur with combination drug studies. It is also worth noting that the presence of strong NLB implies the existence of Loewe synergy (but the reverse does not necessarily hold true, particularly for large differences in relative potency between the two drugs used in combination). For further discussion, see Peterson and Novick (4). Nonetheless, these case studies show

(particularly for the high folic acid experiment) that even if strong NLB is not achieved, it may be possible for one or both of the (combination-to-single-agent) dose ratios to be quite small. This may be useful if it is desirable to use a drug combination to lower the levels of one or both of the drugs to lessen possible adverse reactions.

7. ACKNOWLEDGEMENTS

I would like to acknowledge discussions with Steven Novick and Bill Greco that helped to provide me with further insight on the topic of drug synergy quantification. I would also like to thank the referees and the Managing Editor for their helpful comments.

8. REFERENCES

1. Faessel, H. M., H. K. Slocum, R. C. Jackson, T. J. Boritzki, Y. M. Rustum, M. G. Nair, & W. R. Greco: Super *in vitro* synergy between inhibitors of dihydrofolate reductase and inhibitors of other folate-requiring enzymes: The critical role of polyglutamylation. *Cancer Research* 58, 3036-3050, (1998)
2. Minto, C. F., T. W. Schnider, T. G. Short, K. M. Gregg, A. Gentilini, & S. L. Shafer: Response surface model for

- anesthetic drug interactions , *Anesthesiology*, 92, 1603-1616 (2000)
3. White, D. B., H. K. Slocum, Y. Brun, C. Wrzosek, & W. R. Greco: A new nonlinear mixture response surface paradigm for the study of synergism: A three drug example, *Current Drug Metabolism*, 4, 399-409 (2003)
4. Peterson, J. J. & S. J. Novick: Nonlinear Blending: A useful general concept for the assessment of combination drug synergy , *Journal of Receptors and Signal Transduction* , 27, 125-146 (2007)
5. Bliss C. I.: The Toxicity of poisons combined jointly. *Annals of Applied Biology* 26, 585-615 (1939)
6. Loewe, S.: The problem of Synergism and Antagonism of Combined Drugs , *Arzeim. Forsch.*, 3, 285-290 (1953)
7. Greco, W. R., G. Bravo, G. & J. C. Parsons: The search for synergy: A critical review from a response surface perspective , *Pharmacological Reviews*, 47, 331-385 (1995)
8. Tallarida, R.: *Drug Synergism and Dose-Effect Data Analysis*, Chapman & Hall/CRC, Boca Raton, FL (2000)
9. Berenbaum M. C.: The expected effect of a combination of agents: The general solution, *Journal of Theoretical Biology*, 114, 413-431 (1985)
10. Luszczki, J. J., M. M. Andres, P. Czuczwar, A. Cioczek-Czuczwar, N. Ratnaraj, P. N. Patsalos, & S. J. Czuczwar: Pharmacodynamic and pharmacokinetic characterization of interactions between levetiracetam and numerous antiepileptic drugs in the mouse maximal electroshock seizure model: An isobolographic analysis , *Epilepsia* 47, 10-20 (2006)
11. Lehar, J. & C. Keith: Quantifying the effects of compound combinations , International Union of Pure and Applied Chemistry (IUPAC) Project Description (Project Number: 2003-059-1-700) (2004) available at <http://sunsite.wits.ac.za/iupac/projects/2003/2003-059-1-700.html>
12. Cornell, J. A.: *Experiments with Mixtures : Designs, Models, and the Analysis of Mixture Data*, 3rd ed., John Wiley, New York, NY (2002)
13. Smith, W. F.: *Experimental Design For Formulation*, ASA-SIAM Series on Statistics and Probability, SIAM Philadelphia, PA, ASA, Alexandria, VA (2005)
14. Piepel, G. F. & J. A. Cornell: Models for mixture experiments when the response depends upon the total amount , *Technometrics*, 27, 219-227 (1985)
15. Piepel, G. F. & J. A. Cornell: Designs for mixture-amount experiments , *Journal of Quality Technology*, 19, 11-28 (1987)
16. Claringbold, P. J.: Use of the simplex design in the study of the joint action of related hormones, *Biometrics*, 11, 174-185 (1955)
17. Kitsos, C. P. & L. Edler: *Cancer risk assessment for mixtures* , in *Recent Advances in Quantitative Methods in Cancer and Human Health Risk Assessment*, (Chapter 17) 283-298, John Wiley & Sons, Ltd., Chichester, England (2005)
18. Chen, J. J., R. L. Kodell, & Y. Chen: Designs and models for mixtures: Assessing cumulative risk, in *Recent Advances in Quantitative Methods in Cancer and Human Health Risk Assessment*, (Chapter 18) 299-316, John Wiley & Sons, Ltd., Chichester, England (2005)
19. Greco, W. R., H. Faessel, & L. Levasseur: The search for cytotoxic synergy between anticancer agents: a case of Dorothy and the ruby slippers?, *Journal of the National Cancer Institute*, 88 (11) (1996)
20. Borisy, A. A., P. J. Elliott, N. W. Hurst, M. S. Lee, J. Lehár, E. R. Price, G. Serbedzija, G. R. Zimmermann, M. A. Foley, B. R. Stockwell, & C. T. Keith: Systematic discovery of multicomponent therapeutics. *Proceedings of the National Academy of Sciences*, 100, 7977-7982 (2003)
21. Chou, J. H. and Chou, T. C. (1988) Computerized simulation of dose reduction index (DRI) in synergistic drug combinations. *Pharmacologist* 30:A231.
22. Chou, T. C.: Theoretical basis, experimental design, and computerized simulation of synergism and antagonism in drug combination studies, *Pharmacological Reviews*, 58, 621-681. (2006)
23. Bishop, Y. M. M., S. E. Fienberg, and P. W. Holland, *Discrete Multivariate Analysis*, Cambridge, MA: MIT Press (1975)
24. Silvapulle, M. J. & P. K. Sen: *Constrained Statistical Inference*, John Wiley & Sons, Inc., Hoboken, NJ (2005)
25. Westfall, P. H., S.-Y. Ho, S.-Y., & B. A. Prillaman: Properties of multiple intersection-union tests for multiple endpoints in combination therapy trials , *Journal of Biopharmaceutical Statistics*, 11, 125-138 (2001)
26. Konishi, S. and G. Kitagawa: *Information Criteria and Statistical Modeling*, Springer, New York, NY (2008)
27. Peterson, J. J., S. Cahya, & E. Del Castillo: A general approach to confidence regions for optimal factor levels of response surfaces, *Biometrics*, 58, 422-431 (2002)

Abbreviations: DRP: dose reduction profile, EOHS: excess over highest single agent, MW: Minto-White, mMW: molar-unit Minto-White, NLB: nonlinear blending, TMQ: trimetrexate

Key Words: Antagonism, Berenbaum Interaction Index, Bliss Independence, Coalism, Combination Index, Confidence Region, Dose Reduction Index, Dose Reduction Profile, Dosewise Additivity, Excess Over Highest Single Agent, Isobole, Isobologram, Loewe Synergy, Min Test, Minto-White Model, Nonlinear

Synergy concepts of nonlinear blending and dose-reduction profiles

Blending, Partial Inhibitor, Potentiation, Response Surface, Review, Synergy, Review

Send correspondence to: John J. Peterson, Drug Development Sciences Department, Research Statistics Unit (UP-4315), GlaxoSmithKline Pharmaceuticals, R&D, 1250 So. Collegeville Road, Collegeville, PA, 19426, USA, Tel: 610-917-6242, Fax: 610-917-4818 E-mail: john.peterson@gsk.com

<http://www.bioscience.org/current/vol2S.htm>